Effect of Alaska pollock-gelatin sheet sealant on bonding strength and regeneration of nerve

Ryosuke Tsujisaka, MD[1], Taku Suzuki, MD, PhD[1], Shinsuke Shibata, MD, PhD[2], Takuji Iwamoto, MD, PhD[1], Tetsushi Taguchi, PhD[3,4], Masaya Nakamura, MD, PhD[1]

1. Department of Orthopedic Surgery, Keio University School of Medicine
   35 Shinano-machi, Shinjuku, Tokyo 160-8582, Japan
2. Electron Microscope Laboratory, Keio University School of Medicine
   35 Shinano-machi, Shinjuku, Tokyo 160-8582, Japan
3. Graduate School of Pure and Applied Sciences, University of Tsukuba
   1-1-1 Tennodai, Tsukuba, Ibaraki 305-8577, Japan
4. Polymers and Biomaterials Field, Research Center for Functional Materials, National Institute for Materials Science
   1-1 Namiki, Tsukuba, Ibaraki 305-0044, Japan

Corresponding authors:

Taku Suzuki, MD, PhD

Department of Orthopedic Surgery, Keio University School of Medicine

35 Shinano-machi, Shinjuku-ku, Tokyo 160-8582, Japan

Tel: +81-3-5363-3812

E-mail: sutaku49@gmail.com

Tetsushi Taguchi, PhD

Polymers and Biomaterials Field, Research Center for Functional Materials, National Institute for Materials Science

1-1 Namiki, Tsukuba, Ibaraki 305-0044, Japan

Tel: +81-29-860-4498

Email: TAGUCHI.Tetsushi@nims.go.jp

Keywords: Alaska pollock-gelatin; Alaska pollock-gelatin sealant; Alaska pollock-gelatin sheet; fibrin glue; nerve; sealant

Acknowledgements: We are grateful to Dr. N. Matsumura, N. Nagoshi, and Dr. S. Masuda in Department of Orthopaedic Surgery, Keio University School of Medicine, N. Moritoki in Electron Microscope Laboratory, Keio University School of Medicine, H. Ichimaru, and A. Nishiguchi in Polymers and Biomaterials Field, Research Center for Functional Materials, National Institute for Materials Science for their helpful support. We are grateful to Pro. Y. Kubota and Dr. N. Imanishi for approving the use of the cadavers donated to the Clinical Anatomy Laboratory, Keio University School of Medicine.

Declaration of conflicting interests The authors declared no potential conflicts of interest with respect to the research, authorship, and/or publication of this article.

Funding This work was supported by the Japan Society for the Promotion of Science (JSPS) KAKENHI (Grant No. 22K09364).

Ethical approval Protocols for the cadaver experiments were approved by the Clinical Anatomy Laboratory with the consent of the families (approval no. 20150385), and animal experiments were approved by the Institutional Animal Care and Use Committee of our institution (approval no. A2022-016).

Informed consent The cadavers used in our study were donated to the Clinical Anatomy Laboratory, Keio University School of Medicine, with the consent of the families.

Contributorship details: All authors contributed to the study conception and design. R.T., T.S., S.S., and T.T. performed experimentation and data acquisition. R.T., T.S. and T.T. searched the scientific literature. R.T., T.S., S.S., and T.T. wrote the first draft of the manuscript. T.I., and M.N. revised the manuscript critically for important content. All authors read and approved the final manuscript.

Effect of Alaska pollock-gelatin sheet on repair strength and regeneration of nerve

ABSTRACT

This study aimed to investigate the repair strength and the biocompatibility of Alaska pollock-derived gelatin (ApGltn) sheet for nerve repair. Cadaveric digital nerves were repaired with double suture, single suture + ApGltn sheet, single suture + fibrin glue, single suture, ApGltn sheet, and fibrin, and maximum failure loads were measured (20 nerves each). Rat sciatic nerves were repaired with double suture, single suture + ApGltn sheet, single suture, ApGltn sheet, fibrin glue, and resection (10 nerves each). Macroscopic appearance, muscle weight, and histopathological findings were examined 8 weeks postoperatively. The failure load of ApGltn sheet (0.39 N) was significantly higher than that of a fibrin (0.05 N),and that of single suture + ApGltn sheet (1.32 N) was significantly higher than that of a single suture alone (0.97 N). Functional and histological examinations showed similar recovery among sutures, ApGltn, and fibrin groups. ApGltn sheet is useful for clinical application as an alternative to fibrin.

INTRODUCTION

Acute nerve injury commonly occurs due to upper limb trauma, and primary suture of the nerve is a standard technique for its repair. Some materials, such as fibrin glue (Felix et al., 2013; Rafijah et al., 2013), polyethylene glycol (Bamba et al., 2018; Riley et al., 2015), and laser welding (Barton et al., 2013; Turner et al., 2018), enhance the bonding strength at the repair site (Barton et al., 2014). Among these, fibrin sealant is the most frequently used material at nerve coaptation sites due to its biocompatibility; however, the usefulness of fibrin addition remains controversial due to the lack of bonding strength (Childe et al., 2018; Isaacs et al., 2008; Nishimura et al., 2008; Sameem et al., 2011; Temple et al., 2004; Tse and Ko, 2012).

Recently, a novel biocompatible liquid-type sealant composed of Alaska pollock-derived gelatin (ApGltn), partially modified with various alkyl groups and a polyethylene glycol-based crosslinker, was introduced and demonstrated good burst strength when tested on porcine aorta and rat lungs (Mizuno et al., 2017; Taguchi et al., 2016). The liquid-type ApGltn sealant also showed higher bonding strength and an equal effect on nerve regeneration when compared with the fibrin sealant using the digital nerve in cadaveric models and sciatic nerves in rat models. (Masuda et al., 2021). Furthermore, Taguchi et al. fabricated tissue-adhesive fibre sheets (ApGltn sheet) based on decyl group-modified ApGltn (C10-ApGltn) by the electrospinning method (Ichimaru et al., 2021). The burst strength, defined as the pressure at which the ApGltn sheets sealing the porcine pleura ruptured as water pressure gradually increased, was 108 times higher than that of commercial polyglycolic acid sheets (Ichimaru et al., 2021). Sheet-type adhesive ApGltn sealant may be clinically

Commented [TH1]: You need to make clear in the introduction how this study differs from your previous study:
Masuda S, Suzuki T, Shibata S et al. A novel Alaska pollock gelatin sealant shows higher bonding strength and nerve regeneration comparable to that of fibrin sealant in a cadaveric model and a rat model. Plast Reconstr Surg. 2021, 148: 742e-52e.

Commented [鈴木2R1]: Thank you for your valuable comments. These studies (Mizuno et al., 2017; Taguchi et al., 2016) demonstrated the burst strength of ApGltn sealant using porcine aorta and rat lungs. In contrast, our previous study (Masuda et al., 2021) examined the bonding strength of ApGltn sealant utilizing the digital nerve in cadaveric models and the sciatic nerves in rat models. This distinction has been clarified in lines 31-35 on page 2.

easier to use for nerve repair than the liquid type because it can be stored at room temperature without requiring any special apparatuses (Ichimaru and Taguchi, 2021). The ApGltn sheet is a promising material for enhancing the bonding strength at the nerve repair site. However, whether it can increase the bonding strength when tension is applied to the ruptured site and there is axonal regeneration remains unclear. Therefore, this study aimed to investigate the bonding strength and biocompatibility of this sheet type of sealant in transected digital nerves in a cadaveric model and sciatic nerves in a rat model (Figure S1).

METHODS

In the cadaveric study, all procedures were carried out in accordance with the relevant guidelines and regulations of the Clinical Anatomy Laboratory of our institution. All experimental protocols were approved by the ethics committee (approval no. 20150385). Informed consent was obtained from all participants and/or their legal guardians prior to death. For the animal study, all experimental protocols were approved by Institutional Animal Care and Use Committee of our institution (approval no. A2022-016).

Characteristics and preparation of the sealants

Manufacture of ApGltn sheets (Ichimaru et al., 2021)

C10-ApGltn was synthesized by reductive amination of amino groups in ApGltn with decanal, as previously reported (Mizuno et al., 2017; Taguchi et al., 2016). ApGltn sheets composed of C10-ApGltn were fabricated by electrospinning. Briefly, 0.9 g of C10-ApGltn was dissolved in 3 mL of a 60% aqueous ethanol solution at 55°C. The solution was loaded into a syringe with an 18 G needle and placed in an electrospinning machine (NANON-03, MECC Co., Ltd., Japan). The solution was then extruded at a rate of 1 mL/h and an electrospinning voltage of 22 kV. The ApGltn sheets were collected on silicone-coated aluminum membranes positioned 15 cm from the needle tip. To improve stability under wet conditions, the obtained sheets were thermally cross-linked at 150°C for 5 h under reduced pressure. Sheet thickness was 500μm, and they were bioresorbable within 4 weeks (Figure S2). The microstructure of the fabricated ApGltn sheets was observed using scanning electron microscopy (SEM; JSM-5600, JEOL Ltd., Japan) after sputtering with platinum for 5 min (Figure S2). Thereafter, the ApGltn sheets were stored at room temperature until further use.

Fibrin glue

Fibrin glue (Beliplast P Combi-set, CSL Behring, PA, USA) used in this study was stored in a refrigerator (4 °C) before use. Fibrinogen powder (40 mg) and coagulation factor XIII (30 IU) were dissolved in Aprotinin solution (500 KIE/0.5 ml). Powder of thrombin concentrate (150 IU) was dissolved in calcium chloride solution (2.94 g/0.5 ml). The fibrinogen and the thrombin solutions were cured by mixing equal volumes of each solution.

Traction force testing using a cadaveric model

The primary outcome was the load to failure when traction force was applied to the repaired digital nerves from freshly frozen cadavers. One hundred and twenty digital nerves from six freshly frozen cadavers (mean age: 89 (SD 6) years; three women and three men) were used.

Surgical procedures for digital nerve repair

Digital nerves in a cadaveric model were selected, because our preliminary experiment showed that the sciatic nerve size in mice or rats was too small for clamping to the traction machine (Masuda et al., 2021). All surgical procedures were performed by a single-hand surgeon, according to a previously reported method (Masuda et al., 2021). Radial and ulnar digital nerves (6 cm length) were harvested from all five digits.

Each nerve segment was cut transversely at its midpoint. The nerves were repaired using six techniques (20 nerves per group): (a) double suture, (b) single suture + ApGltn sheet, (c) single suture + fibrin sealant, (d) single suture, (e) ApGltn sheet, and (f) fibrin sealant. To compare the failure load using similar size nerves, the same cadavers were used for procedures (a) and (c), for (b) and (d), and for (e) and (f). Digital nerves from the right hand were used for procedures (a), (b), and (e) and those from the left hand for (c), (d), and (f). In procedures (a), (b), (c), and (d), the transected nerve was repaired with a single- or double-epineural suture using an 8-0 monofilament nylon suture (Crownjun KONO, Tokyo, Japan). In procedures (b) and (e), an ApGltn sheet of approximately 10 × 15 mm was

placed around the nerve repair site (Figure 1). In procedures (c) and (f), approximately 1 ml of fibrin sealant was applied around the repair. The glue sleeve length was five times the width of the nerve itself.

Biomechanical evaluation

Biomechanical strength was tested 5 to 10 min postoperatively, according to a previously described method (Masuda et al., 2021). Approximately 1 cm segments of the proximal and distal nerve ends were clamped to a material testing machine (Table-top Material Tensile Tester; EZ Graph, Shimadzu Corporation, Kyoto, Japan) with a load range of 100 N. Nerves were pulled uniaxially at a rate of 5 mm/min until terminal rupture occurred. The peak recorded load was considered as the maximum failure load.

Functional evaluation using a rat model

The secondary outcome was the functional recovery of the repaired sciatic nerve using a rat model. To prepare a sciatic-nerve injury model, 53 eight-week-old male Wistar rats (Sankyo Labo, Tokyo, Japan) with a mean body weight of 198 (182–224) g at the time of surgery were used.

Surgical procedures for nerve repair

All rats were deeply anaesthetized with intraperitoneal ketamine (90 mg/kg; Sankyo, Tokyo, Japan) and xylazine (10 mg/kg; Bayer, Leverkusen, Germany). The left leg was used as the experimental limb, and the right leg was used for sham operation, or as a control. A dorsal longitudinal skin incision was made, and the sciatic nerve was exposed by splitting the gluteal muscle. The nerves were treated with seven surgical interventions: (a) double suture, (b) single suture + ApGltn sheet, (c) single suture, (d) ApGltn sheet, (e) fibrin sealant, (f) resection of the nerve with a 5-mm segmental defect, and (g) sham (placebo) operation (10 nerves each for [a] to [f] and three nerves for [g]). Procedures employing suture + fibrin sealant was not performed in the rat model, since the results of biomechanical traction testing showed that there was no significant difference between the procedures employing suture and those employing suture + fibrin sealant. In procedures (a)–(f), the sciatic nerve segment was cut transversely at the midpoint of the nerve. In procedures (a)–(c), the transected nerve was repaired with a single- or double-epineural suture using a 9-0 monofilament nylon suture (Crownjun KONO, Tokyo, Japan). In procedures (b) and (d), ApGltn sheet of approximately 10 × 5 mm was placed around the nerve division site. In procedures (e), approximately 0.1 ml of fibrin adhesive was placed around the nerve rupture site. When the ApGltn sheet and fibrin sealant were applied to the nerve, a plastic sheet was laid beneath the nerve to avoid adherence of the sealant to the nerve bed. During the sham operations, sciatic nerves were explored without damaging them. After surgery, the treated limbs were not immobilized, and the rats were allowed unrestricted motion.

To evaluate nerve regeneration, walking track analysis was performed every two weeks until 8 weeks after the procedure, when macroscopic examination, muscle weight measurement, and histological examination were conducted.

Macroscopic examination

The sciatic nerve was exposed using a procedure similar to that described previously. The macroscopic appearance of the sciatic nerve, including nerve continuity and ApGltn sheet absorption, was confirmed. Nerve continuity was defined as complete continuity (continuity with normal nerve thickness), incomplete continuity (continuity with nerve narrowing), or complete rupture (visible separation at the coaptation site) (Masuda et al., 2021).

Muscle weight measurement

Both tibialis anterior muscles were harvested and weighed. Muscle recovery was calculated by comparing the weights of the experimental and control limbs.

Walking track analysis

Walking track analysis was performed to evaluate motor function. Rats were placed on a treadmill, and their footprints were scanned using the DigiGait System (Rat Specifics, MA, USA).

153 The sciatic functional index (SFI) was calculated according to a previously reported formula (Bain et
154 al., 1989). The zero value of the SFI denotes normal nerve function, and a value of −100 represents
155 total loss of nerve function.
156
157 *Histological examination*
158 Three out of ten sciatic nerves from each group were examined histologically. To assess the
159 histological changes in the axons and myelin sheaths, specimens from the sciatic nerves 3 mm distal
160 to the repair site in each group were obtained for electron and light microscopy (Kimura et al., 2018;
161 Shibata et al., 2015). Semi-thin sections of 1 μm thickness were stained with 0.1% toluidine blue for
162 7 min and imaged using a BZ-X700 optical microscope (Keyence, Osaka, Japan). Ultrathin axial
163 sections (70 nm thickness) of the sciatic nerve were prepared using an ultramicrotome (Leica UC7,
164 Leica Microsystems GmbH, Wetzlar, Germany) on silicon wafers and stained with uranyl acetate and
165 lead citrate for 10 min. The sections were observed under a SU6600 SEM (Hitachi High-Tech, Tokyo,
166 Japan) by detecting backscattered electrons with an acceleration voltage of 5 kV. For quantitative
167 analysis, axonal density was used to evaluate the regenerated nerve fibres. Axonal density was
168 defined as axonal area/total area, and myelin sheath density was defined as myelin sheath area/total
169 area in a fascicle in each nerve sample (Takagi et al., 2009). For G-ratio quantification, 300 fibres
170 (100 from each nerve) randomly selected from electron microscopy images were used.
171
172 ***Statistical analysis***

The Shapiro-Wilk test was used to assess the normality of data. Data are presented as mean with standard error. To evaluate intergroup differences, one-way analysis of variance (ANOVA) with Tukey or Games-Howell post hoc comparisons were used for maximum failure load, muscle weight, and axonal density analysis. The Kruskal–Wallis and Dann–Bonferroni tests for post hoc comparisons were used for axon diameter analyses. Two-way repeated ANOVA was used for the comparison between SFI values. Statistical analysis was performed by a hand surgeon who was blinded to clinical information. Post-hoc power analysis was conducted to confirm whether this sample size would be adequate to detect a significant difference, with an alpha of 0.05. Effect sizes are expressed as mean values with standard deviations. The power analysis demonstrated statistical powers of 100%, 97%, 98%, and 100% for the cadaveric model, muscle weight, SFI, and G-ratio, respectively. Statistical significance was set at $p < 0.05$.

RESULTS

Failure load using the cadaveric model

The maximum failure load for each procedure is shown in figure 2. The maximum failure load of ApGltn sheet was significantly higher than that of a fibrin sealant (0.39 N vs. 0.05 N, $p < 0.001$). The maximum failure load of single suture + ApGltn sheet was significantly higher than that of a single suture (1.32 N vs. 0.97 N, $p = 0.02$). There were no significant differences between single suture + fibrin sealant and single suture (0.99 N vs. 0.97 N, $p = 0.99$). The double suture technique

193 (1.65 N) had a higher maximum failure load than the single suture + ApGltn sheet technique, but this
194 was not significant ($p = 0.07$). The maximum failure load of the ApGltn sheet (0.39 N) and fibrin
195 sealant (0.05 N) was significantly lower than those of the other four procedures ($p < 0.001$).
196
197 ***Functional evaluation using the rat model***
198 *Macroscopic examination*
199 All resected sciatic nerves in the double suture, single suture + ApGltn sheet, single suture, and
200 ApGltn sheet groups showed complete nerve continuity without defects. The ApGltn sheets were
201 resorbed and had disappeared by 8 weeks after the initial procedure. Fibrin groups showed complete
202 continuity of the nerves in 9 rats and incomplete continuity in 1 rat. In the resection group, complete
203 rupture was observed in five of ten rats, complete continuity in two, and incomplete continuity in
204 three rats (Figure S3).
205
206 *Muscle weight*
207 Muscle weight recovery did not significantly differ among the double suture, single suture +
208 ApGltn sheet, single suture, ApGltn sheet, and fibrin techniques ($p > 0.05$) (Figure 3). However, a
209 significant difference was observed between the resection group and the double suture, single suture
210 + ApGltn sheet, single suture, and ApGltn sheet groups ($p < 0.05$).
211

Walking track analysis

SFI improved over time; the double suture and single suture + ApGltn sheet groups showed significantly higher SFI values than the ApGltn sheet, single suture, fibrin, and resection groups ($p < 0.05$) (Figure 4). The ApGltn sheet groups showed significantly higher SFI values than the resection group ($p < 0.05$).

Histological examination

Optical and electron microscopy images of the toluidine blue-stained nerves fibre are shown in figure 5. In axial sections, a larger number of myelinated axons were observed in the double suture, single suture + ApGltn sheet, single suture, ApGltn sheet, and fibrin groups than in the resection group. Quantitative analysis of the axonal density indicated that the double suture and single suture + ApGltn sheet groups had significantly higher values than the fibrin group (Figure 6). No significant differences were observed in axonal density among the double suture, single suture + ApGltn sheet, ApGltn sheet, and single suture groups.

The G-ratios are shown in figure S4. Although the double suture group showed thicker myelin regeneration than the single suture + ApGltn sheet group (Figure S4a), the axonal diameters did not significantly differ between the two groups (Figure S5). Similar axonal regrowth patterns were observed in the single suture + ApGltn sheet and single suture groups (Figure S4b) and the single suture and ApGltn sheet groups (Figure S4c); the axonal diameters among the three groups did not significantly differ (Figure S5). The ApGltn sheet group showed thicker myelin regeneration than the

fibrin group (Figure S4d). The axonal diameters indicated that the double suture, single suture + ApGltn sheet, single suture, and ApGltn sheet groups had significantly higher values than the fibrin group.

DISCUSSION

In this study, the bonding strength and functional recovery of transected nerves using ApGltn sheets were compared with traditional sutures and fibrin sealant in cadaveric and rat models. The maximum failure load of the ApGltn sheet was approximately eight times higher than that of the fibrin sealant. Although the bonding strength of the ApGltn sheet was inferior to that of the traditional suture, the addition of the ApGltn sheet to the single suture significantly reinforced the repair strength. Addition of fibrin sealant to the single suture did not significantly reinforce the strength. The ApGltn sheet did not compromise sciatic nerve regeneration compared with the traditional suture.

Liquid ApGltn sealant has a stronger breaking strength than fibrin sealant (Masuda et al., 2021; Mizuno et al., 2017; Taguchi et al., 2016; Yamaoka et al., 2019). Taguchi et al. (2016) demonstrated that the burst strength of the ApGltn sealant was 11.6 times higher than that of a fibrin sealant in a burst porcine aorta model (341 vs. 29 mm Hg). Additionally, Masuda et al. (2021) showed that the maximum failure load of liquid-type ApGltn sealant was approximately three times higher than that of the fibrin sealant using a cadaveric digital nerve model (0.22 versus 0.06 N). Although a direct comparison between that study and ours is difficult due to the different digital nerve sizes from

different specimens employed, the breaking strength of the ApGltn sheet (0.39 N) is higher than that of the liquid-type ApGltn sealant. However, the failure load of the ApGltn sheet was inferior to that of the traditional suture, as also shown in a previous report on liquid ApGltn sealant (Masuda et al., 2021).

To minimize the effect of size differences, a previous cadaveric model similar to our study compared bilateral digital nerves from the same specimen (Masuda et al., 2021). Addition of liquid ApGltn sealant to the single suture did not significantly increase the maximum failure load (mean 0.1 N) compared to the single suture (Masuda et al., 2021); therefore, they concluded that liquid ApGltn sealant with the reported bonding strength cannot be used clinically, and further improvement of the strength in the ApGltn sealant is required. Our study showed that the addition of an ApGltn sheet to a single suture does significantly reinforce the bonding strength (mean 0.35 N). Fibrin glue is sometimes added to the nerve suture site (Isaacs, 2010); however, our results are consistent with the previous findings that the addition of fibrin glues does not significantly increase the maximum failure load (Isaacs et al., 2008). The ApGltn sealant, compared to the fibrin sealant, has been shown to have prolonged adhesive capacity and reduced viral infection risk and cost (Nishimura et al., 2008; Taguchi et al., 2016). Since ApGltn is derived from the waste product of Alaska pollack skin, the cost of materials could be quite low. Therefore, ApGltn sheets could be clinically useful in the future as an alternative to fibrin sealants.

In the present study, sciatic nerves repaired with sheet-type ApGltn sealant showed nerve recovery similar to that in the suture group. This result is consistent with that of a previous study

using liquid ApGltn sealant, showing similar nerve recovery compared to suture and fibrin sealant repair in a rat sciatic nerve model (Masuda et al., 2021). Furthermore, sheet-type ApGltn sealants completely degrade within 21 days without severe inflammation when subcutaneously implanted in the backs of rats (Ichimaru et al., 2021). In an in vitro study, ApGltn sheet had excellent cytocompatibility and efficiently supported the growth of L929 cells (Ichimaru and Taguchi, 2021). Moreover, since it is composed of gelatin, ApGltn sheets do not prevent tissue regeneration.

In addition to the bonding strength, the ApGltn sheet has other advantages over liquid ApGltn sealant. Liquid-type adhesives need to mix two components homogeneously; therefore, they require special apparatuses to rapidly mix the components during surgery (Mizuno et al., 2017). Sheet-type adhesives have been developed for their easy sealing property without any special apparatus. Additionally, the liquid type requires refrigeration before use, whereas the sheet type can be stored at room temperature. Furthermore, liquid-type adhesives are difficult to apply evenly around the entire circumference of the suture site in clinical practice, whereas the sheet-type are more evenly applied. Altogether, the ApGltn sheet is clinically easier to use for nerve repair than the liquid type.

Our study had some limitations. The maximum failure load of a repaired nerve could differ according to the digital nerve size. To minimize the effect of size differences, the same cadavers were used for the single suture + ApGltn sheet (b) and single suture procedures (d); the double suture (a) and single suture + fibrin sealant (c) procedures; and ApGltn sheet (e) and fibrin sealant (f) procedures. However, the different cadavers used for the procedures might have affected the results. Nerve regeneration was studied in an animal model only. Therefore, clinical trials are needed to validate the

application of this sealant in humans.

In conclusion, the maximum failure load of the ApGltn sheet was higher than that of the fibrin sealant. Addition of the ApGltn sheet to a single suture significantly reinforces the repair strength of the nerve. Its effect on transected nerve regeneration is similar to that of the traditional suture. Although ApGltn sheet cannot serve as a substitute for sutures, we believe that addition of ApGltn sheets to the nerve suture site will be useful for clinical application in the future as an alternative to fibrin sealant.

REFERENCES

Bain JR, Mackinnon SE, Hunter DA. Functional evaluation of complete sciatic, peroneal, and posterior tibial nerve lesions in the rat. Plast Reconstr Surg. 1989, 83: 129-38.

Bamba R, Riley DC, Kim JS et al. Evaluation of a nerve fusion technique with polyethylene glycol in a delayed setting after nerve injury. J Hand Surg Am. 2018, 43: 82.e1-.e7.

Barton M, Morley JW, Stoodley MA et al. Laser-activated adhesive films for sutureless median nerve anastomosis. J Biophotonics. 2013, 6: 938-49.

Barton MJ, Morley JW, Stoodley MA, Lauto A, Mahns DA. Nerve repair: Toward a sutureless approach. Neurosurg Rev. 2014, 37: 585-95.

Childe JR, Regal S, Schimoler P, Kharlamov A, Miller MC, Tang P. Fibrin glue increases the tensile strength of conduit-assisted primary digital nerve repair. Hand (N Y). 2018, 13: 45-9.

313 Felix SP, Pereira Lopes FR, Marques SA, Martinez AM. Comparison between suture and fibrin glue
314 on repair by direct coaptation or tubulization of injured mouse sciatic nerve. Microsurgery. 2013, 33:
315 468-77.
316 Ichimaru H, Mizuno Y, Chen X, Nishiguchi A, Taguchi T. Prevention of pulmonary air leaks using a
317 biodegradable tissue-adhesive fibre sheet based on alaska pollock gelatin modified with decanyl
318 groups. Biomater Sci. 2021, 9: 861-73.
319 Ichimaru H, Taguchi T. Improved tissue adhesion property of a hydrophobically modified alaska
320 pollock derived gelatin sheet by uv treatment. Int J Biol Macromol. 2021, 172: 580-8.
321 Isaacs J. Treatment of acute peripheral nerve injuries: Current concepts. J Hand Surg Am. 2010, 35:
322 491-7.
323 Isaacs JE, McDaniel CO, Owen JR, Wayne JS. Comparative analysis of biomechanical performance
324 of available "nerve glues". J Hand Surg Am. 2008, 33: 893-9.
325 Kimura H, Ouchi T, Shibata S et al. Stem cells purified from human induced pluripotent stem cell-
326 derived neural crest-like cells promote peripheral nerve regeneration. Sci Rep. 2018, 8: 10071.
327 Masuda S, Suzuki T, Shibata S et al. A novel Alaska pollock gelatin sealant shows higher bonding
328 strength and nerve regeneration comparable to that of fibrin sealant in a cadaveric model and a rat
329 model. Plast Reconstr Surg. 2021, 148: 742e-52e.
330 Mizuno Y, Mizuta R, Hashizume M, Taguchi T. Enhanced sealing strength of a hydrophobically-
331 modified alaska pollock gelatin-based sealant. Biomater Sci. 2017, 5: 982-9.
332 Mizuno Y, Taguchi T. Promotion of cell migration into a hydrophobically modified alaska pollock

gelatin-based hydrogel. Macromol Biosci. 2019, 19: e1900083.

Mizuta R, Taguchi T. Enhanced sealing by hydrophobic modification of alaska pollock-derived gelatin-based surgical sealants for the treatment of pulmonary air leaks. Macromol Biosci. 2017, 17.

Nishimura MT, Mazzer N, Barbieri CH, Moro CA. Mechanical resistance of peripheral nerve repair with biological glue and with conventional suture at different postoperative times. J Reconstr Microsurg. 2008, 24: 327-32.

Rafijah G, Bowen AJ, Dolores C, Vitali R, Mozaffar T, Gupta R. The effects of adjuvant fibrin sealant on the surgical repair of segmental nerve defects in an animal model. J Hand Surg Am. 2013, 38: 847-55.

Riley DC, Bittner GD, Mikesh M et al. Polyethylene glycol-fused allografts produce rapid behavioral recovery after ablation of sciatic nerve segments. J Neurosci Res. 2015, 93: 572-83.

Sameem M, Wood TJ, Bain JR. A systematic review on the use of fibrin glue for peripheral nerve repair. Plast Reconstr Surg. 2011, 127: 2381-90.

Shibata S, Murota Y, Nishimoto Y et al. Immuno-electron microscopy and electron microscopic in situ hybridization for visualizing pirna biogenesis bodies in drosophila ovaries. Methods Mol Biol. 2015, 1328: 163-78.

Taguchi T, Ryo M, Ito T, Yoshizawa K, Kajiyama M. Robust sealing of blood vessels with cholesteryl group-modified, alaska pollock-derived gelatin-based biodegradable sealant under wet conditions. J Biomed Nanotechnol. 2016, 12: 128-34.

Takagi T, Nakamura M, Yamada M et al. Visualization of peripheral nerve degeneration and

regeneration: Monitoring with diffusion tensor tractography. Neuroimage. 2009, 44: 884-92.

Temple CL, Ross DC, Dunning CE, Johnson JA. Resistance to disruption and gapping of peripheral nerve repairs: An in vitro biomechanical assessment of techniques. J Reconstr Microsurg. 2004, 20: 645-50.

Tse R, Ko JH. Nerve glue for upper extremity reconstruction. Hand Clin. 2012, 28: 529-40.

Turner NJ, Johnson SA, Foster LJR, Badylak SF. Sutureless nerve repair with ecm bioscaffolds and laser-activated chitosan adhesive. J Biomed Mater Res B Appl Biomater. 2018, 106: 1698-711.

Yamaoka M, Maki N, Wijesinghe A et al. Novel alaska pollock gelatin sealant shows high adhesive quality and conformability. Ann Thorac Surg. 2019, 107: 1656-62.

FIGURE LEGENDS

Figure 1. Resected digital nerves repaired with single suture + ApGltn sheet. An approximately 10 × 15 mm sheet was applied around the nerve rupture site.

Figure 2. The maximum failure load for each procedure. The failure load of the single suture + ApGltn sheet was significantly higher than that of the single suture and that of ApGltn sheet was significantly higher than that of a fibrin sealant. Each box represents the interquartile range of values,

with the bold line showing the median value. The vertical lines show maximum and minimum values. *p < 0.05, **p < 0.001

Figure 3. Muscle weight recovery of the tibialis anterior in the experimental limbs compared with that in the control limbs. No significant differences are observed among the procedures employing double sutures, single sutures + ApGltn sheets, single sutures, ApGltn sheets, and fibrin techniques. Each box represents the interquartile range of values, with the bold line showing the median value. The vertical lines show maximum and minimum values. *p < 0.05, **p < 0.001

Figure 4. Sciatic functional index in each procedure until the completion of 8 postoperative weeks at 4, 6, and 8 weeks, the double suture and single suture + ApGltn sheet groups show significantly higher values than the ApGltn sheet, single suture, fibrin, and resection groups. Data are presented as mean with standard deviation.

Figure 5. Axial sections of the sciatic nerve: light microscopy with toluidine blue (above) and electron microscopy with uranyl acetate (below) staining. A larger number of myelinated axons are observed in the double suture, single suture + ApGltn sheet, single suture, ApGltn sheet, fibrin groups than in the negative control resection group.

Figure 6. Quantitative analysis of axonal density of the regenerated nerve fibrefibres. The double suture and single suture + ApGltn sheet groups had significantly higher values than the fibrin sealant. No significant differences were observed among the double suture, single suture + ApGltn sheet, ApGltn sheet, and single suture. Each box represents the interquartile range of values, with the bold line showing the median value. The vertical lines show maximum and minimum values. *$p < 0.05$, **$p < 0.001$

Figure S1. Biomechanical traction testing using transected digital nerves in a cadaveric model and functional testing using transected sciatic nerves in a rat model.

Figure S2. Photograph of prepared ApGltn sheet (left) and scanning electron microscopy images of ApGltn sheet (right).

Figure S3. Macroscopic examination of the resected sciatic nerves. All resected sciatic nerves in the double suture, single suture + ApGltn sheet, single suture, ApGltn sheet, and fibrin groups show nerve continuity, while segmental defects are observed in five out of ten rats in the resection group.

Figure S4. The G-ratio and axon diameter results. The approximate linear regression equation for each group is shown in the graph.

(a) Double suture and single suture + ApGltn sheet

(b) Single suture + ApGltn sheet and single suture

(c) Single suture and ApGltn sheet

(d) ApGltn sheet and fibrin sealant

Figure S5. Axonal diameter of the regenerated nerve fibres. The axonal diameters indicated that the double suture, single suture + ApGltn sheet, single suture, and ApGltn sheet groups had significantly higher values than the fibrin group. Each box represents the interquartile range of values, with the bold line showing the median value. The vertical lines show maximum and minimum values. *$p < 0.05$, **$p < 0.001$

Effect of Alaska pollock-gelatin sheet on repair strength and regeneration of nerve

ABSTRACT

This study aimed to investigate the repair strength and the biocompatibility of Alaska pollock-derived gelatin (ApGltn) sheet for nerve repair. Cadaveric digital nerves were repaired with double suture, single suture + ApGltn sheet, single suture + fibrin glue, single suture, ApGltn sheet, and fibrin, and maximum failure loads were measured (20 nerves each). Rat sciatic nerves were repaired with double suture, single suture + ApGltn sheet, single suture, ApGltn sheet, fibrin glue, and resection (10 nerves each). Macroscopic appearance, muscle weight, and histopathological findings were examined 8 weeks postoperatively. The failure load of ApGltn sheet (0.39 N) was significantly higher than that of a fibrin (0.05 N),and that of single suture + ApGltn sheet (1.32 N) was significantly higher than that of a single suture alone (0.97 N). Functional and histological examinations showed similar recovery among sutures, ApGltn, and fibrin groups. ApGltn sheet is useful for clinical application as an alternative to fibrin.

INTRODUCTION

Acute nerve injury commonly occurs due to upper limb trauma, and primary suture of the nerve is a standard technique for its repair. Some materials, such as fibrin glue (Felix et al., 2013; Rafijah et al., 2013), polyethylene glycol (Bamba et al., 2018; Riley et al., 2015), and laser welding (Barton et al., 2013; Turner et al., 2018), enhance the bonding strength at the repair site (Barton et al., 2014). Among these, fibrin sealant is the most frequently used material at nerve coaptation sites due to its biocompatibility; however, the usefulness of fibrin addition remains controversial due to the lack of bonding strength (Childe et al., 2018; Isaacs et al., 2008; Nishimura et al., 2008; Sameem et al., 2011; Temple et al., 2004; Tse and Ko, 2012).

Recently, a novel biocompatible liquid-type sealant composed of Alaska pollock-derived gelatin (ApGltn), partially modified with various alkyl groups and a polyethylene glycol-based crosslinker, was introduced and demonstrated good burst strength when tested on porcine aorta and rat lungs (Mizuno et al., 2017; Taguchi et al., 2016). The liquid-type ApGltn sealant also showed higher bonding strength and an equal effect on nerve regeneration when compared with the fibrin sealant using the digital nerve in cadaveric models and sciatic nerves in rat models. (Masuda et al., 2021). Furthermore, Taguchi et al. fabricated tissue-adhesive fibre sheets (ApGltn sheet) based on decyl group-modified ApGltn (C10-ApGltn) by the electrospinning method (Ichimaru et al., 2021). The burst strength, defined as the pressure at which the ApGltn sheets sealing the porcine pleura ruptured as water pressure gradually increased, was 108 times higher than that of commercial polyglycolic acid sheets (Ichimaru et al., 2021). Sheet-type adhesive ApGltn sealant may be clinically

easier to use for nerve repair than the liquid type because it can be stored at room temperature without requiring any special apparatuses (Ichimaru and Taguchi, 2021). The ApGltn sheet is a promising material for enhancing the bonding strength at the nerve repair site. However, whether it can increase the bonding strength when tension is applied to the ruptured site and there is axonal regeneration remains unclear. Therefore, this study aimed to investigate the bonding strength and biocompatibility of this sheet type of sealant in transected digital nerves in a cadaveric model and sciatic nerves in a rat model (Figure S1).

METHODS

In the cadaveric study, all procedures were carried out in accordance with the relevant guidelines and regulations of the Clinical Anatomy Laboratory of our institution. All experimental protocols were approved by the ethics committee (approval no. 20150385). Informed consent was obtained from all participants and/or their legal guardians prior to death. For the animal study, all experimental protocols were approved by Institutional Animal Care and Use Committee of our institution (approval no. A2022-016).

Characteristics and preparation of the sealants

Manufacture of ApGltn sheets (Ichimaru et al., 2021)

C10-ApGltn was synthesized by reductive amination of amino groups in ApGltn with decanal, as previously reported (Mizuno et al., 2017; Taguchi et al., 2016). ApGltn sheets composed of C10-ApGltn were fabricated by electrospinning. Briefly, 0.9 g of C10-ApGltn was dissolved in 3 mL of a 60% aqueous ethanol solution at 55°C. The solution was loaded into a syringe with an 18 G needle and placed in an electrospinning machine (NANON-03, MECC Co., Ltd., Japan). The solution was then extruded at a rate of 1 mL/h and an electrospinning voltage of 22 kV. The ApGltn sheets were collected on silicone-coated aluminum membranes positioned 15 cm from the needle tip. To improve stability under wet conditions, the obtained sheets were thermally cross-linked at 150°C for 5 h under reduced pressure. Sheet thickness was 500μm, and they were bioresorbable within 4 weeks (Figure S2). The microstructure of the fabricated ApGltn sheets was observed using scanning electron microscopy (SEM; JSM-5600, JEOL Ltd., Japan) after sputtering with platinum for 5 min (Figure S2). Thereafter, the ApGltn sheets were stored at room temperature until further use.

Fibrin glue

Fibrin glue (Beliplast P Combi-set, CSL Behring, PA, USA) used in this study was stored in a refrigerator (4 °C) before use. Fibrinogen powder (40 mg) and coagulation factor XIII (30 IU) were dissolved in Aprotinin solution (500 KIE/0.5 ml). Powder of thrombin concentrate (150 IU) was dissolved in calcium chloride solution (2.94 g/0.5 ml). The fibrinogen and the thrombin solutions were cured by mixing equal volumes of each solution.

78

79 ***Traction force testing using a cadaveric model***

80 The primary outcome was the load to failure when traction force was applied to the repaired
81 digital nerves from freshly frozen cadavers. One hundred and twenty digital nerves from six freshly
82 frozen cadavers (mean age: 89 (SD 6) years; three women and three men) were used.

83

84 *Surgical procedures for digital nerve repair*

85 Digital nerves in a cadaveric model were selected, because our preliminary experiment showed
86 that the sciatic nerve size in mice or rats was too small for clamping to the traction machine (Masuda
87 et al., 2021). All surgical procedures were performed by a single-hand surgeon, according to a
88 previously reported method (Masuda et al., 2021). Radial and ulnar digital nerves (6 cm length) were
89 harvested from all five digits.

90 Each nerve segment was cut transversely at its midpoint. The nerves were repaired using six
91 techniques (20 nerves per group): (a) double suture, (b) single suture + ApGltn sheet, (c) single suture
92 + fibrin sealant, (d) single suture, (e) ApGltn sheet, and (f) fibrin sealant. To compare the failure load
93 using similar size nerves, the same cadavers were used for procedures (a) and (c), for (b) and (d), and
94 for (e) and (f). Digital nerves from the right hand were used for procedures (a), (b), and (e) and those
95 from the left hand for (c), (d), and (f). In procedures (a), (b), (c), and (d), the transected nerve was
96 repaired with a single- or double-epineural suture using an 8-0 monofilament nylon suture (Crownjun
97 KONO, Tokyo, Japan). In procedures (b) and (e), an ApGltn sheet of approximately 10 × 15 mm was

placed around the nerve repair site (Figure 1). In procedures (c) and (f), approximately 1 ml of fibrin sealant was applied around the repair. The glue sleeve length was five times the width of the nerve itself.

Biomechanical evaluation

Biomechanical strength was tested 5 to 10 min postoperatively, according to a previously described method (Masuda et al., 2021). Approximately 1 cm segments of the proximal and distal nerve ends were clamped to a material testing machine (Table-top Material Tensile Tester; EZ Graph, Shimadzu Corporation, Kyoto, Japan) with a load range of 100 N. Nerves were pulled uniaxially at a rate of 5 mm/min until terminal rupture occurred. The peak recorded load was considered as the maximum failure load.

Functional evaluation using a rat model

The secondary outcome was the functional recovery of the repaired sciatic nerve using a rat model. To prepare a sciatic-nerve injury model, 53 eight-week-old male Wistar rats (Sankyo Labo, Tokyo, Japan) with a mean body weight of 198 (182–224) g at the time of surgery were used.

Surgical procedures for nerve repair

All rats were deeply anaesthetized with intraperitoneal ketamine (90 mg/kg; Sankyo, Tokyo, Japan) and xylazine (10 mg/kg; Bayer, Leverkusen, Germany). The left leg was used as the experimental limb, and the right leg was used for sham operation, or as a control. A dorsal longitudinal skin incision was made, and the sciatic nerve was exposed by splitting the gluteal muscle. The nerves were treated with seven surgical interventions: (a) double suture, (b) single suture + ApGltn sheet, (c) single suture, (d) ApGltn sheet, (e) fibrin sealant, (f) resection of the nerve with a 5-mm segmental defect, and (g) sham (placebo) operation (10 nerves each for [a] to [f] and three nerves for [g]). Procedures employing suture + fibrin sealant was not performed in the rat model, since the results of biomechanical traction testing showed that there was no significant difference between the procedures employing suture and those employing suture + fibrin sealant. In procedures (a)–(f), the sciatic nerve segment was cut transversely at the midpoint of the nerve. In procedures (a)–(c), the transected nerve was repaired with a single- or double-epineural suture using a 9-0 monofilament nylon suture (Crownjun KONO, Tokyo, Japan). In procedures (b) and (d), ApGltn sheet of approximately 10 × 5 mm was placed around the nerve division site. In procedures (e), approximately 0.1 ml of fibrin adhesive was placed around the nerve rupture site. When the ApGltn sheet and fibrin sealant were applied to the nerve, a plastic sheet was laid beneath the nerve to avoid adherence of the sealant to the nerve bed. During the sham operations, sciatic nerves were explored without damaging them. After surgery, the treated limbs were not immobilized, and the rats were allowed unrestricted motion.

To evaluate nerve regeneration, walking track analysis was performed every two weeks until 8 weeks after the procedure, when macroscopic examination, muscle weight measurement, and histological examination were conducted.

Macroscopic examination

The sciatic nerve was exposed using a procedure similar to that described previously. The macroscopic appearance of the sciatic nerve, including nerve continuity and ApGltn sheet absorption, was confirmed. Nerve continuity was defined as complete continuity (continuity with normal nerve thickness), incomplete continuity (continuity with nerve narrowing), or complete rupture (visible separation at the coaptation site) (Masuda et al., 2021).

Muscle weight measurement

Both tibialis anterior muscles were harvested and weighed. Muscle recovery was calculated by comparing the weights of the experimental and control limbs.

Walking track analysis

Walking track analysis was performed to evaluate motor function. Rats were placed on a treadmill, and their footprints were scanned using the DigiGait System (Rat Specifics, MA, USA).

153 The sciatic functional index (SFI) was calculated according to a previously reported formula (Bain et
154 al., 1989). The zero value of the SFI denotes normal nerve function, and a value of −100 represents
155 total loss of nerve function.
156
157 *Histological examination*
158 Three out of ten sciatic nerves from each group were examined histologically. To assess the
159 histological changes in the axons and myelin sheaths, specimens from the sciatic nerves 3 mm distal
160 to the repair site in each group were obtained for electron and light microscopy (Kimura et al., 2018;
161 Shibata et al., 2015). Semi-thin sections of 1 μm thickness were stained with 0.1% toluidine blue for
162 7 min and imaged using a BZ-X700 optical microscope (Keyence, Osaka, Japan). Ultrathin axial
163 sections (70 nm thickness) of the sciatic nerve were prepared using an ultramicrotome (Leica UC7,
164 Leica Microsystems GmbH, Wetzlar, Germany) on silicon wafers and stained with uranyl acetate and
165 lead citrate for 10 min. The sections were observed under a SU6600 SEM (Hitachi High-Tech, Tokyo,
166 Japan) by detecting backscattered electrons with an acceleration voltage of 5 kV. For quantitative
167 analysis, axonal density was used to evaluate the regenerated nerve fibres. Axonal density was
168 defined as axonal area/total area, and myelin sheath density was defined as myelin sheath area/total
169 area in a fascicle in each nerve sample (Takagi et al., 2009). For G-ratio quantification, 300 fibres
170 (100 from each nerve) randomly selected from electron microscopy images were used.
171
172 ***Statistical analysis***

The Shapiro-Wilk test was used to assess the normality of data. Data are presented as mean with standard error. To evaluate intergroup differences, one-way analysis of variance (ANOVA) with Tukey or Games-Howell post hoc comparisons were used for maximum failure load, muscle weight, and axonal density analysis. The Kruskal–Wallis and Dann–Bonferroni tests for post hoc comparisons were used for axon diameter analyses. Two-way repeated ANOVA was used for the comparison between SFI values. Statistical analysis was performed by a hand surgeon who was blinded to clinical information. Post-hoc power analysis was conducted to confirm whether this sample size would be adequate to detect a significant difference, with an alpha of 0.05. Effect sizes are expressed as mean values with standard deviations. The power analysis demonstrated statistical powers of 100%, 97%, 98%, and 100% for the cadaveric model, muscle weight, SFI, and G-ratio, respectively. Statistical significance was set at $p < 0.05$.

RESULTS

Failure load using the cadaveric model

The maximum failure load for each procedure is shown in figure 2. The maximum failure load of ApGltn sheet was significantly higher than that of a fibrin sealant (0.39 N vs. 0.05 N, $p < 0.001$). The maximum failure load of single suture + ApGltn sheet was significantly higher than that of a single suture (1.32 N vs. 0.97 N, $p = 0.02$). There were no significant differences between single suture + fibrin sealant and single suture (0.99 N vs. 0.97 N, $p = 0.99$). The double suture technique

193 (1.65 N) had a higher maximum failure load than the single suture + ApGltn sheet technique, but this
194 was not significant ($p = 0.07$). The maximum failure load of the ApGltn sheet (0.39 N) and fibrin
195 sealant (0.05 N) was significantly lower than those of the other four procedures ($p < 0.001$).
196
197 ***Functional evaluation using the rat model***
198 *Macroscopic examination*
199 All resected sciatic nerves in the double suture, single suture + ApGltn sheet, single suture, and
200 ApGltn sheet groups showed complete nerve continuity without defects. The ApGltn sheets were
201 resorbed and had disappeared by 8 weeks after the initial procedure. Fibrin groups showed complete
202 continuity of the nerves in 9 rats and incomplete continuity in 1 rat. In the resection group, complete
203 rupture was observed in five of ten rats, complete continuity in two, and incomplete continuity in
204 three rats (Figure S3).
205
206 *Muscle weight*
207 Muscle weight recovery did not significantly differ among the double suture, single suture +
208 ApGltn sheet, single suture, ApGltn sheet, and fibrin techniques ($p > 0.05$) (Figure 3). However, a
209 significant difference was observed between the resection group and the double suture, single suture
210 + ApGltn sheet, single suture, and ApGltn sheet groups ($p < 0.05$).
211

212 *Walking track analysis*

213 SFI improved over time; the double suture and single suture + ApGltn sheet groups showed
214 significantly higher SFI values than the ApGltn sheet, single suture, fibrin, and resection groups ($p <$
215 0.05) (Figure 4). The ApGltn sheet groups showed significantly higher SFI values than the resection
216 group ($p < 0.05$).

217

218 *Histological examination*

219 Optical and electron microscopy images of the toluidine blue-stained nerves fibre are shown in
220 figure 5. In axial sections, a larger number of myelinated axons were observed in the double suture,
221 single suture + ApGltn sheet, single suture, ApGltn sheet, and fibrin groups than in the resection
222 group. Quantitative analysis of the axonal density indicated that the double suture and single suture
223 + ApGltn sheet groups had significantly higher values than the fibrin group (Figure 6). No significant
224 differences were observed in axonal density among the double suture, single suture + ApGltn sheet,
225 ApGltn sheet, and single suture groups.

226 The G-ratios are shown in figure S4. Although the double suture group showed thicker myelin
227 regeneration than the single suture + ApGltn sheet group (Figure S4a), the axonal diameters did not
228 significantly differ between the two groups (Figure S5). Similar axonal regrowth patterns were
229 observed in the single suture + ApGltn sheet and single suture groups (Figure S4b) and the single
230 suture and ApGltn sheet groups (Figure S4c); the axonal diameters among the three groups did not
231 significantly differ (Figure S5). The ApGltn sheet group showed thicker myelin regeneration than the

fibrin group (Figure S4d). The axonal diameters indicated that the double suture, single suture + ApGltn sheet, single suture, and ApGltn sheet groups had significantly higher values than the fibrin group.

DISCUSSION

In this study, the bonding strength and functional recovery of transected nerves using ApGltn sheets were compared with traditional sutures and fibrin sealant in cadaveric and rat models. The maximum failure load of the ApGltn sheet was approximately eight times higher than that of the fibrin sealant. Although the bonding strength of the ApGltn sheet was inferior to that of the traditional suture, the addition of the ApGltn sheet to the single suture significantly reinforced the repair strength. Addition of fibrin sealant to the single suture did not significantly reinforce the strength. The ApGltn sheet did not compromise sciatic nerve regeneration compared with the traditional suture.

Liquid ApGltn sealant has a stronger breaking strength than fibrin sealant (Masuda et al., 2021; Mizuno et al., 2017; Taguchi et al., 2016; Yamaoka et al., 2019). Taguchi et al. (2016) demonstrated that the burst strength of the ApGltn sealant was 11.6 times higher than that of a fibrin sealant in a burst porcine aorta model (341 vs. 29 mm Hg). Additionally, Masuda et al. (2021) showed that the maximum failure load of liquid-type ApGltn sealant was approximately three times higher than that of the fibrin sealant using a cadaveric digital nerve model (0.22 versus 0.06 N). Although a direct comparison between that study and ours is difficult due to the different digital nerve sizes from

252 different specimens employed, the breaking strength of the ApGltn sheet (0.39 N) is higher than that
253 of the liquid-type ApGltn sealant. However, the failure load of the ApGltn sheet was inferior to that
254 of the traditional suture, as also shown in a previous report on liquid ApGltn sealant (Masuda et al.,
255 2021).

256 To minimize the effect of size differences, a previous cadaveric model similar to our study
257 compared bilateral digital nerves from the same specimen (Masuda et al., 2021). Addition of liquid
258 ApGltn sealant to the single suture did not significantly increase the maximum failure load (mean 0.1
259 N) compared to the single suture (Masuda et al., 2021); therefore, they concluded that liquid ApGltn
260 sealant with the reported bonding strength cannot be used clinically, and further improvement of the
261 strength in the ApGltn sealant is required. Our study showed that the addition of an ApGltn sheet to
262 a single suture does significantly reinforce the bonding strength (mean 0.35 N). Fibrin glue is
263 sometimes added to the nerve suture site (Isaacs, 2010); however, our results are consistent with the
264 previous findings that the addition of fibrin glues does not significantly increase the maximum failure
265 load (Isaacs et al., 2008). The ApGltn sealant, compared to the fibrin sealant, has been shown to have
266 prolonged adhesive capacity and reduced viral infection risk and cost (Nishimura et al., 2008; Taguchi
267 et al., 2016). Since ApGltn is derived from the waste product of Alaska pollack skin, the cost of
268 materials could be quite low. Therefore, ApGltn sheets could be clinically useful in the future as an
269 alternative to fibrin sealants.

270 In the present study, sciatic nerves repaired with sheet-type ApGltn sealant showed nerve
271 recovery similar to that in the suture group. This result is consistent with that of a previous study

using liquid ApGltn sealant, showing similar nerve recovery compared to suture and fibrin sealant repair in a rat sciatic nerve model (Masuda et al., 2021). Furthermore, sheet-type ApGltn sealants completely degrade within 21 days without severe inflammation when subcutaneously implanted in the backs of rats (Ichimaru et al., 2021). In an in vitro study, ApGltn sheet had excellent cytocompatibility and efficiently supported the growth of L929 cells (Ichimaru and Taguchi, 2021). Moreover, since it is composed of gelatin, ApGltn sheets do not prevent tissue regeneration.

In addition to the bonding strength, the ApGltn sheet has other advantages over liquid ApGltn sealant. Liquid-type adhesives need to mix two components homogeneously; therefore, they require special apparatuses to rapidly mix the components during surgery (Mizuno et al., 2017). Sheet-type adhesives have been developed for their easy sealing property without any special apparatus. Additionally, the liquid type requires refrigeration before use, whereas the sheet type can be stored at room temperature. Furthermore, liquid-type adhesives are difficult to apply evenly around the entire circumference of the suture site in clinical practice, whereas the sheet-type are more evenly applied. Altogether, the ApGltn sheet is clinically easier to use for nerve repair than the liquid type.

Our study had some limitations. The maximum failure load of a repaired nerve could differ according to the digital nerve size. To minimize the effect of size differences, the same cadavers were used for the single suture + ApGltn sheet (b) and single suture procedures (d); the double suture (a) and single suture + fibrin sealant (c) procedures; and ApGltn sheet (e) and fibrin sealant (f) procedures. However, the different cadavers used for the procedures might have affected the results. Nerve regeneration was studied in an animal model only. Therefore, clinical trials are needed to validate the

application of this sealant in humans.

In conclusion, the maximum failure load of the ApGltn sheet was higher than that of the fibrin sealant. Addition of the ApGltn sheet to a single suture significantly reinforces the repair strength of the nerve. Its effect on transected nerve regeneration is similar to that of the traditional suture. Although ApGltn sheet cannot serve as a substitute for sutures, we believe that addition of ApGltn sheets to the nerve suture site will be useful for clinical application in the future as an alternative to fibrin sealant.

REFERENCES

Bain JR, Mackinnon SE, Hunter DA. Functional evaluation of complete sciatic, peroneal, and posterior tibial nerve lesions in the rat. Plast Reconstr Surg. 1989, 83: 129-38.

Bamba R, Riley DC, Kim JS et al. Evaluation of a nerve fusion technique with polyethylene glycol in a delayed setting after nerve injury. J Hand Surg Am. 2018, 43: 82.e1-.e7.

Barton M, Morley JW, Stoodley MA et al. Laser-activated adhesive films for sutureless median nerve anastomosis. J Biophotonics. 2013, 6: 938-49.

Barton MJ, Morley JW, Stoodley MA, Lauto A, Mahns DA. Nerve repair: Toward a sutureless approach. Neurosurg Rev. 2014, 37: 585-95.

Childe JR, Regal S, Schimoler P, Kharlamov A, Miller MC, Tang P. Fibrin glue increases the tensile strength of conduit-assisted primary digital nerve repair. Hand (N Y). 2018, 13: 45-9.

313 Felix SP, Pereira Lopes FR, Marques SA, Martinez AM. Comparison between suture and fibrin glue
314 on repair by direct coaptation or tubulization of injured mouse sciatic nerve. Microsurgery. 2013, 33:
315 468-77.
316 Ichimaru H, Mizuno Y, Chen X, Nishiguchi A, Taguchi T. Prevention of pulmonary air leaks using a
317 biodegradable tissue-adhesive fibre sheet based on alaska pollock gelatin modified with decanyl
318 groups. Biomater Sci. 2021, 9: 861-73.
319 Ichimaru H, Taguchi T. Improved tissue adhesion property of a hydrophobically modified alaska
320 pollock derived gelatin sheet by uv treatment. Int J Biol Macromol. 2021, 172: 580-8.
321 Isaacs J. Treatment of acute peripheral nerve injuries: Current concepts. J Hand Surg Am. 2010, 35:
322 491-7.
323 Isaacs JE, McDaniel CO, Owen JR, Wayne JS. Comparative analysis of biomechanical performance
324 of available "nerve glues". J Hand Surg Am. 2008, 33: 893-9.
325 Kimura H, Ouchi T, Shibata S et al. Stem cells purified from human induced pluripotent stem cell-
326 derived neural crest-like cells promote peripheral nerve regeneration. Sci Rep. 2018, 8: 10071.
327 Masuda S, Suzuki T, Shibata S et al. A novel Alaska pollock gelatin sealant shows higher bonding
328 strength and nerve regeneration comparable to that of fibrin sealant in a cadaveric model and a rat
329 model. Plast Reconstr Surg. 2021, 148: 742e-52e.
330 Mizuno Y, Mizuta R, Hashizume M, Taguchi T. Enhanced sealing strength of a hydrophobically-
331 modified alaska pollock gelatin-based sealant. Biomater Sci. 2017, 5: 982-9.
332 Mizuno Y, Taguchi T. Promotion of cell migration into a hydrophobically modified alaska pollock

333 gelatin-based hydrogel. Macromol Biosci. 2019, 19: e1900083.

334 Mizuta R, Taguchi T. Enhanced sealing by hydrophobic modification of alaska pollock-derived
335 gelatin-based surgical sealants for the treatment of pulmonary air leaks. Macromol Biosci. 2017, 17.

336 Nishimura MT, Mazzer N, Barbieri CH, Moro CA. Mechanical resistance of peripheral nerve repair
337 with biological glue and with conventional suture at different postoperative times. J Reconstr
338 Microsurg. 2008, 24: 327-32.

339 Rafijah G, Bowen AJ, Dolores C, Vitali R, Mozaffar T, Gupta R. The effects of adjuvant fibrin sealant
340 on the surgical repair of segmental nerve defects in an animal model. J Hand Surg Am. 2013, 38: 847-
341 55.

342 Riley DC, Bittner GD, Mikesh M et al. Polyethylene glycol-fused allografts produce rapid behavioral
343 recovery after ablation of sciatic nerve segments. J Neurosci Res. 2015, 93: 572-83.

344 Sameem M, Wood TJ, Bain JR. A systematic review on the use of fibrin glue for peripheral nerve
345 repair. Plast Reconstr Surg. 2011, 127: 2381-90.

346 Shibata S, Murota Y, Nishimoto Y et al. Immuno-electron microscopy and electron microscopic in
347 situ hybridization for visualizing pirna biogenesis bodies in drosophila ovaries. Methods Mol Biol.
348 2015, 1328: 163-78.

349 Taguchi T, Ryo M, Ito T, Yoshizawa K, Kajiyama M. Robust sealing of blood vessels with cholesteryl
350 group-modified, alaska pollock-derived gelatin-based biodegradable sealant under wet conditions. J
351 Biomed Nanotechnol. 2016, 12: 128-34.

352 Takagi T, Nakamura M, Yamada M et al. Visualization of peripheral nerve degeneration and

353 regeneration: Monitoring with diffusion tensor tractography. Neuroimage. 2009, 44: 884-92.
354 Temple CL, Ross DC, Dunning CE, Johnson JA. Resistance to disruption and gapping of peripheral
355 nerve repairs: An in vitro biomechanical assessment of techniques. J Reconstr Microsurg. 2004, 20:
356 645-50.
357 Tse R, Ko JH. Nerve glue for upper extremity reconstruction. Hand Clin. 2012, 28: 529-40.
358 Turner NJ, Johnson SA, Foster LJR, Badylak SF. Sutureless nerve repair with ecm bioscaffolds and
359 laser-activated chitosan adhesive. J Biomed Mater Res B Appl Biomater. 2018, 106: 1698-711.
360 Yamaoka M, Maki N, Wijesinghe A et al. Novel alaska pollock gelatin sealant shows high adhesive
361 quality and conformability. Ann Thorac Surg. 2019, 107: 1656-62.
362
363
364
365
366 **FIGURE LEGENDS**
367 **Figure 1.** Resected digital nerves repaired with single suture + ApGltn sheet. An approximately 10 ×
368 15 mm sheet was applied around the nerve rupture site.
369
370 **Figure 2.** The maximum failure load for each procedure. The failure load of the single suture +
371 ApGltn sheet was significantly higher than that of the single suture and that of ApGltn sheet was
372 significantly higher than that of a fibrin sealant. Each box represents the interquartile range of values,

with the bold line showing the median value. The vertical lines show maximum and minimum values. *p < 0.05, **p < 0.001

Figure 3. Muscle weight recovery of the tibialis anterior in the experimental limbs compared with that in the control limbs. No significant differences are observed among the procedures employing double sutures, single sutures + ApGltn sheets, single sutures, ApGltn sheets, and fibrin techniques. Each box represents the interquartile range of values, with the bold line showing the median value. The vertical lines show maximum and minimum values. *p < 0.05, **p < 0.001

Figure 4. Sciatic functional index in each procedure until the completion of 8 postoperative weeks at 4, 6, and 8 weeks, the double suture and single suture + ApGltn sheet groups show significantly higher values than the ApGltn sheet, single suture, fibrin, and resection groups. Data are presented as mean with standard deviation.

Figure 5. Axial sections of the sciatic nerve: light microscopy with toluidine blue (above) and electron microscopy with uranyl acetate (below) staining. A larger number of myelinated axons are observed in the double suture, single suture + ApGltn sheet, single suture, ApGltn sheet, fibrin groups than in the negative control resection group.

392 **Figure 6.** Quantitative analysis of axonal density of the regenerated nerve fibrefibres. The double
393 suture and single suture + ApGltn sheet groups had significantly higher values than the fibrin sealant.
394 No significant differences were observed among the double suture, single suture + ApGltn sheet,
395 ApGltn sheet, and single suture. Each box represents the interquartile range of values, with the bold
396 line showing the median value. The vertical lines show maximum and minimum values. *$p < 0.05$,
397 **$p < 0.001$

398

399 **Figure S1.** Biomechanical traction testing using transected digital nerves in a cadaveric model and
400 functional testing using transected sciatic nerves in a rat model.

401

402 **Figure S2.** Photograph of prepared ApGltn sheet (left) and scanning electron microscopy images of
403 ApGltn sheet (right).

404

405 **Figure S3.** Macroscopic examination of the resected sciatic nerves. All resected sciatic nerves in the
406 double suture, single suture + ApGltn sheet, single suture, ApGltn sheet, and fibrin groups show nerve
407 continuity, while segmental defects are observed in five out of ten rats in the resection group.

408

409 **Figure S4.** The G-ratio and axon diameter results. The approximate linear regression equation for
410 each group is shown in the graph.

411 (a) Double suture and single suture + ApGltn sheet

412 (b) Single suture + ApGltn sheet and single suture

413 (c) Single suture and ApGltn sheet

414 (d) ApGltn sheet and fibrin sealant

415

416 **Figure S5.** Axonal diameter of the regenerated nerve fibres. The axonal diameters indicated that the

417 double suture, single suture + ApGltn sheet, single suture, and ApGltn sheet groups had significantly

418 higher values than the fibrin group. Each box represents the interquartile range of values, with the

419 bold line showing the median value. The vertical lines show maximum and minimum values. *$p <$

420 0.05, **$p < 0.001$

421

Figure1

Click here to access/download;Figure(s);Figure1.jpg

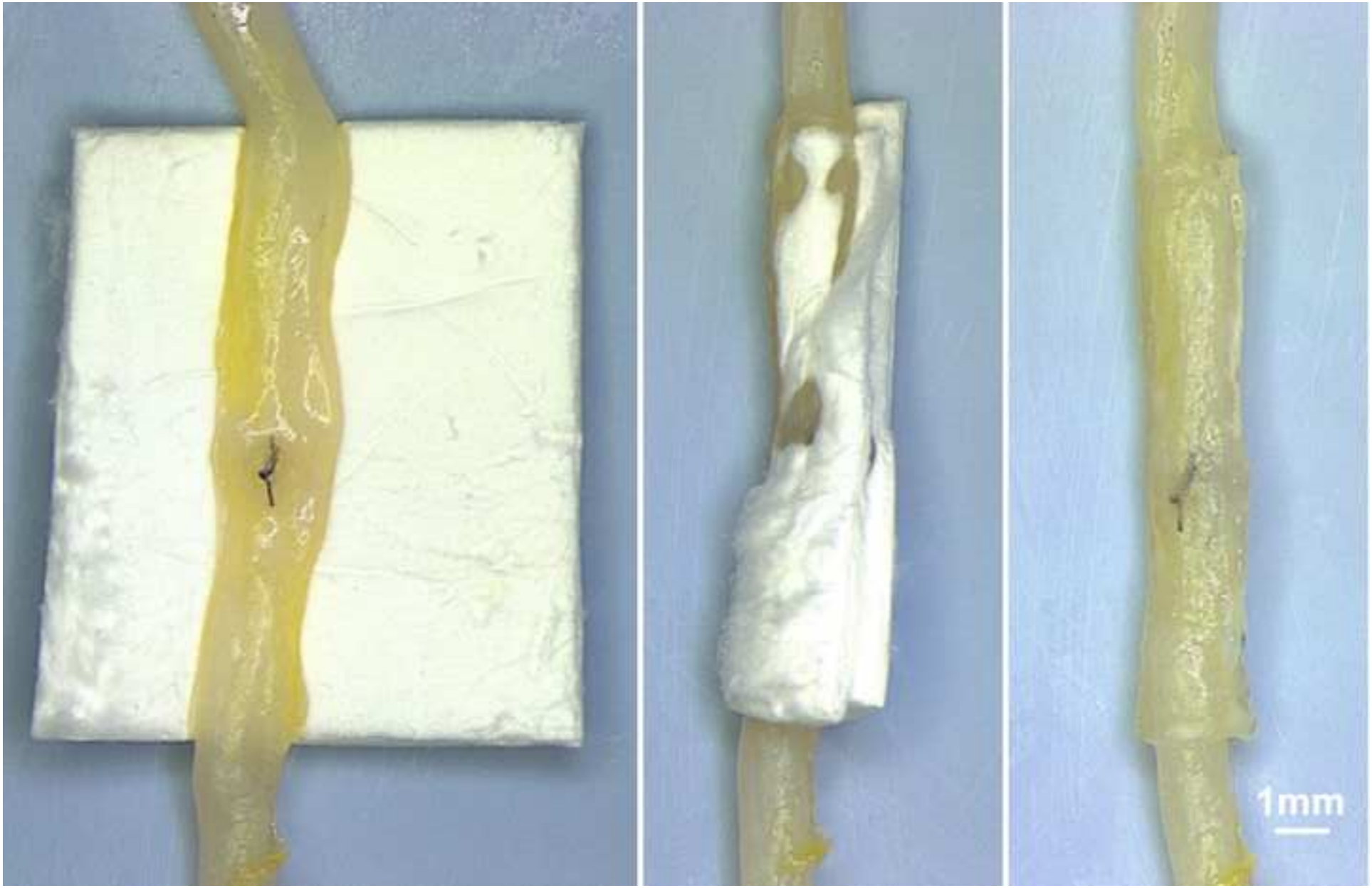

Figure2

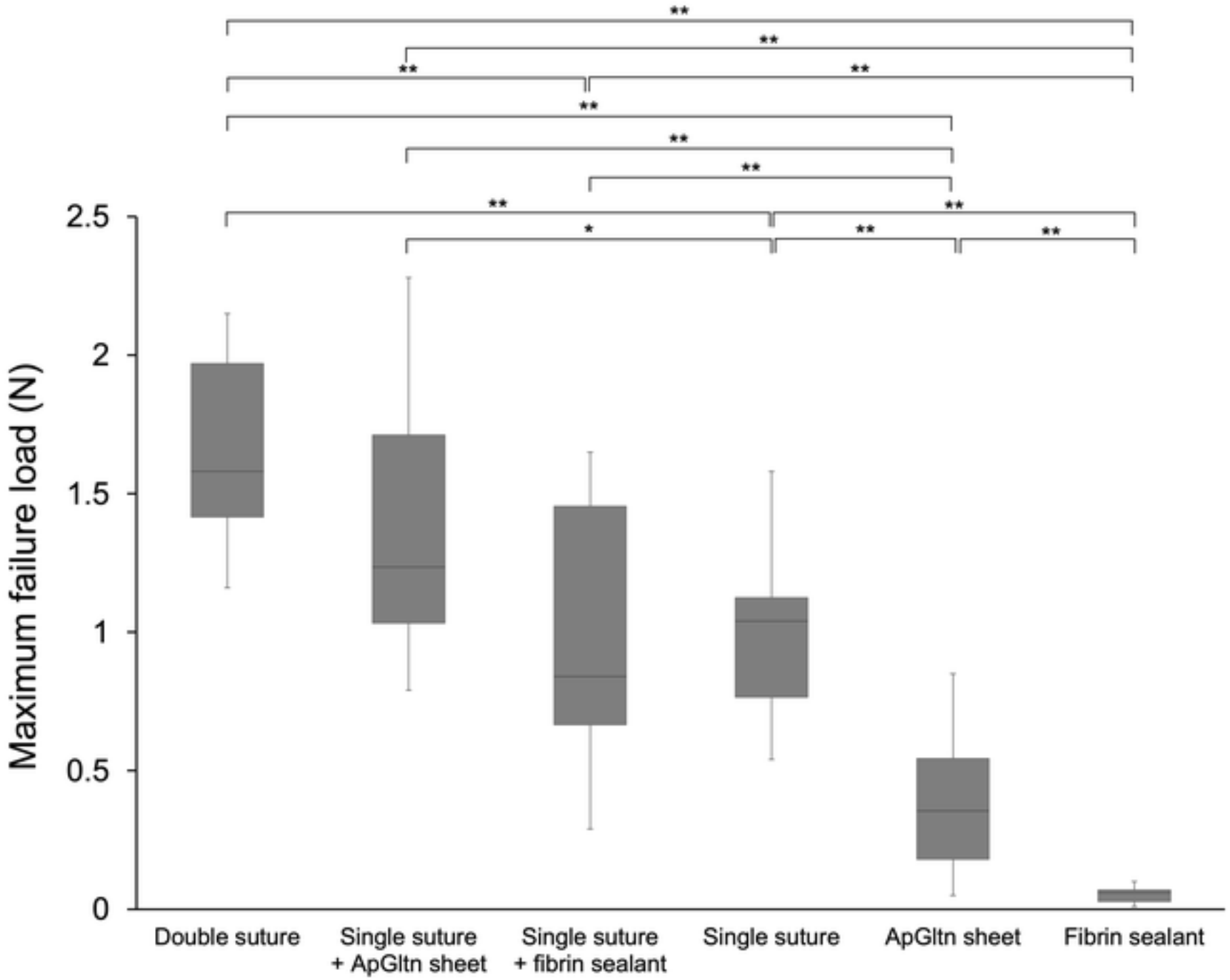

Figure3

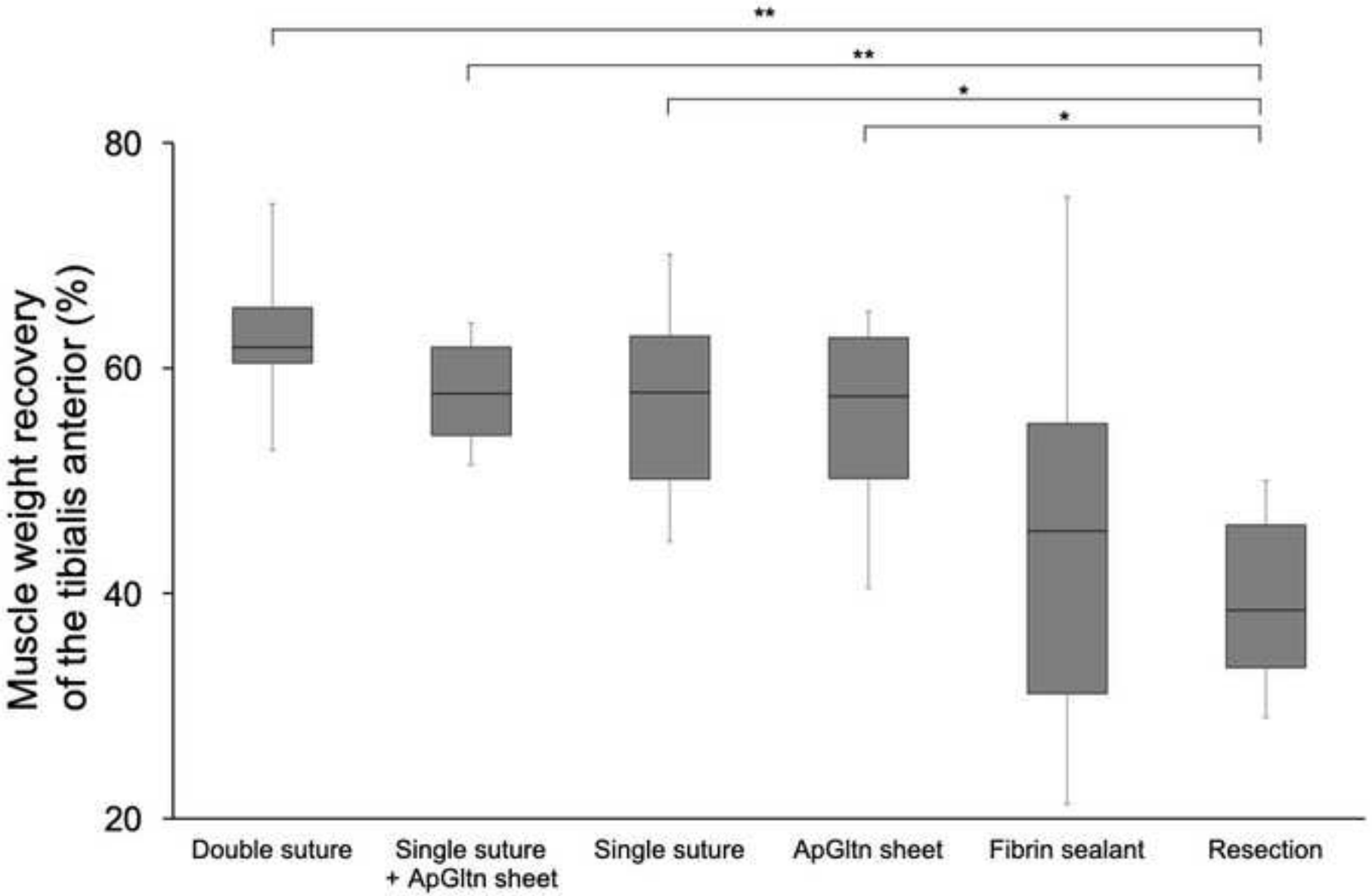

Figure4

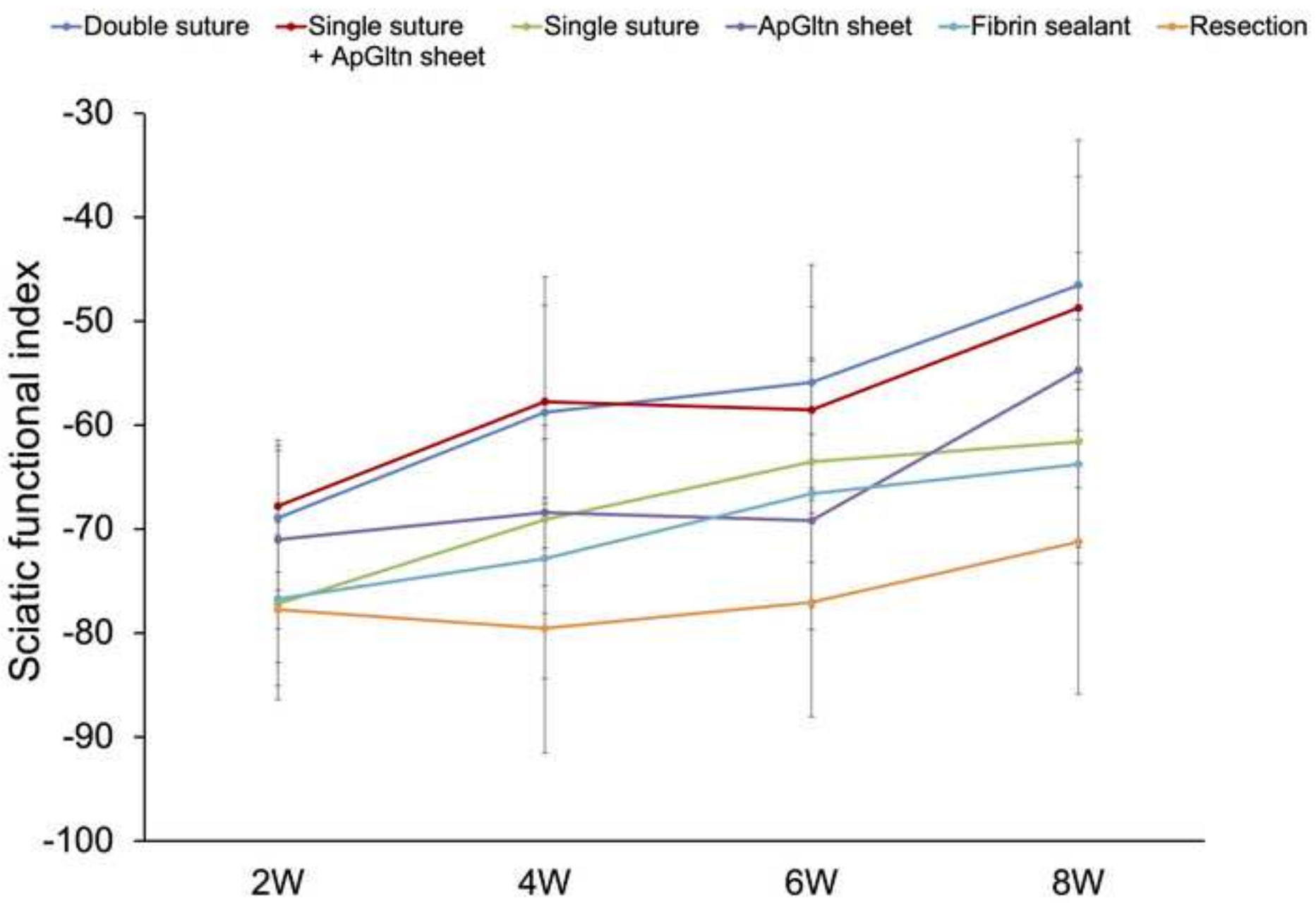

Figure5

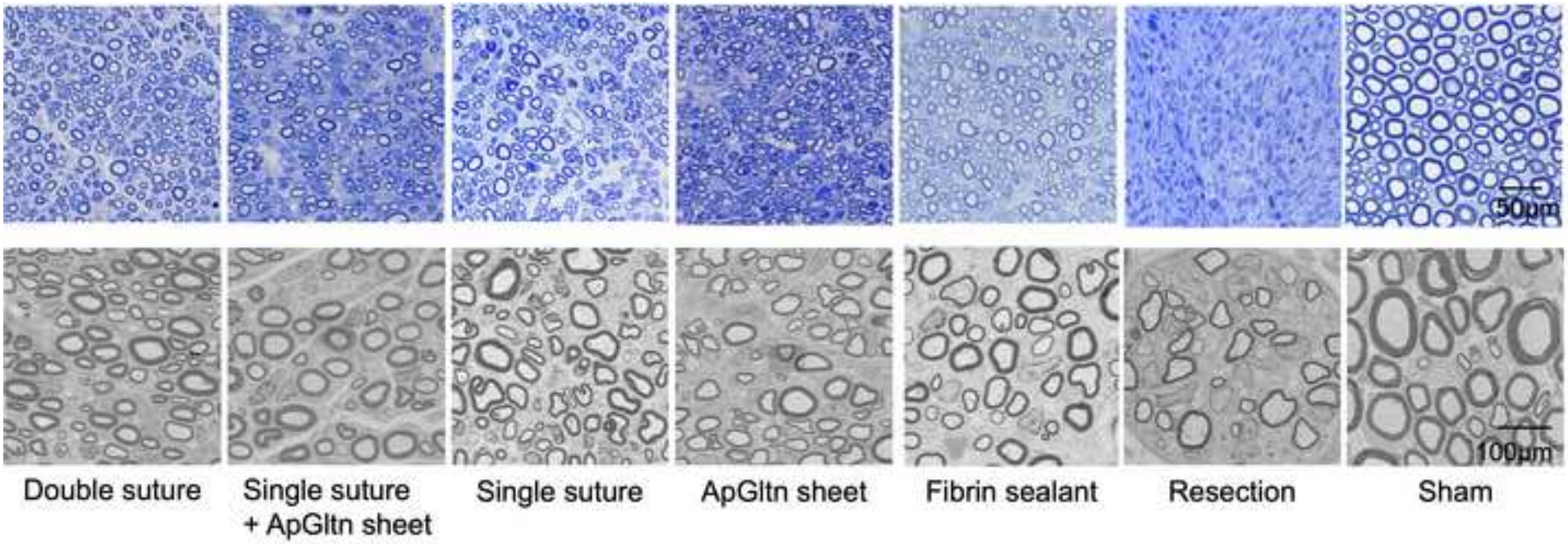

Figure6